

# Dynamics of Interacting Quintessence Models: Observational Constraints

Germán Olivares\*,<sup>1</sup> Fernando Atrio-Barandela†,<sup>2</sup> and Diego Pavón‡<sup>1</sup>

<sup>1</sup>*Departamento de Física, Universidad Autónoma de Barcelona, Barcelona, Spain*

<sup>2</sup>*Departamento de Física Fundamental, Universidad de Salamanca, Spain*

Interacting quintessence models have been proposed to explain or, at least, alleviate the coincidence problem of late cosmic acceleration. In this paper we are concerned with two aspects of these kind of models: (i) the dynamical evolution of the model of Chimento *et al.* [L.P. Chimento, A.S. Jakubi, D. Pavón, and W. Zimdahl, Phys. Rev. D **67**, 083513 (2003).], i.e., whether its cosmological evolution gives rise to a right sequence of radiation, dark matter and dark energy dominated eras, and (ii) whether the dark matter dark energy ratio asymptotically evolves towards a non-zero constant. After showing that the model correctly reproduces these eras, we correlate three data sets that constrain the interaction at three redshift epochs:  $z \leq 10^4$ ,  $z = 10^3$ , and  $z = 1$ . We discuss the model selection and argue that even if the model under consideration fulfills both requirements, it is heavily constrained by observation. The prospects that the coincidence problem can be explained by the coupling of dark matter to dark energy are not clearly favored by the data.

## I. INTRODUCTION

Recent measurements of luminosity distances using supernovae type Ia (SNIa) [1], of the cosmic microwave background (CMB) temperature anisotropies with the Wilkinson Microwave Anisotropy (WMAP) satellite [2], large scale structure [3], the integrated Sachs–Wolfe effect [4], and weak lensing [5], strongly suggest that the Universe is currently undergoing a phase of accelerated expansion -see [6] for recent reviews. Within general relativity the obvious candidate to explain the present acceleration is the cosmological constant (or vacuum energy), and in fact the naïve model built on it,  $\Lambda$ CDM, seems to pass reasonably well all cosmological tests. However, it suffers from two serious drawbacks from the theoretical side: the unnatural low value of the corresponding energy density, 123 magnitude orders larger than observed, and the so-called “coincidence problem”, namely, “Why are the densities of matter and vacuum of the same order precisely today?”, that requires the vacuum energy density to be 96 orders of magnitude smaller than the matter density at the Planck scale. (It is fair, however, to mention the existence of proposals in which a vacuum energy density of about the right order of magnitude stems from the Casimir effect at cosmic scales -see [7] and references therein). This is why much attention has been devoted to models featuring an evolving and nearly un-clustered form of energy, usually dubbed “dark energy”, possessing a strong negative pressure high enough to drive late acceleration -see [8] for an ample review of models.

For simplicity, most cosmological models assume that matter and dark energy interact gravitationally only. In the absence of an underlying symmetry that would suppress a matter-dark energy coupling (or interaction) there is no a priori reason to dismiss it. Further, the coupling is not only likely but inevitable [9] and its introduction is not more arbitrary than assuming it to vanish. On the other hand, it may help explain the coincidence problem. Ultimately, this question will have to be resolved observationally. Among other things, the interaction can push the beginning of the era of accelerated expansion to higher redshifts and it may erroneously suggest (if the interaction is ignored when interpreting the data) an equation of state for the dark energy of phantom type -see [10] and references therein. Another question, is the form of the coupling. There is no clear consensus on this point and different versions, that arise from a variety of motivations, coexist in the literature.

Cosmological models where dark matter (DM) and dark energy (DE) do not evolve separately but interact with each other were first introduced to justify the small current value of the cosmological constant [11] and

---

\* E-mail address: german.olivares@uab.es

† E-mail address: atrio@usal.es

‡ E-mail address: diego.pavon@uab.es

nowadays there is a growing body of literature on the subject -see, e.g. [12] and references therein. Recently, various proposals at the fundamental level, including field Lagrangians, have been advanced to account for the coupling [13]. Lagrangians of scalar field coupled to matter generically do not generate scaling solutions with a dark matter dominated period lasting long enough as required by cosmic structure formation [14].

In this paper we compare the interacting quintessence model (IQM) of Chimento *et al.* [15] (see also its forerunner [16]) with observational data (supernovae, cosmic microwave background (CMB), and matter power spectrum) to set limits on the strength of the interaction DM/DE. The model was built to simultaneously account for the late phase of acceleration in the framework of Einstein relativity and significantly alleviates the coincidence problem. It evades the limits set in [14] and is compatible with a right succession of cosmic eras - radiation, dark matter, and dark energy dominated expansions. In a recent paper, Guo *et al.* also set constraints on interacting quintessence models [17]. However, the interactions studied by these authors differ from the one in [15], and while they use the cosmic background shift parameter and baryon acoustic oscillations alongside supernovae data to constrain the interaction, they do not consider the matter power spectrum, whereby our analysis may be viewed as complementary to theirs.

The outline of this paper is as follows. Next section studies the critical points of the autonomous system of equations associated to the IQM [15]. Section III considers the restrictions set by Amendola *et al.* on the model to conclude that the latter evades these restrictions and, in particular, that an early epoch of baryon dominance is possible only if the strength of interaction is unnaturally large (beyond the limits set by the CMB data). Section IV focus on the observational bounds coming from the CMB, matter power spectrum and recent supernovae type Ia data. Finally, section V summarizes our results.

## II. DYNAMICS OF THE INTERACTING QUINTESSENCE MODEL

If the quintessence DE decays into DM, both energy densities evolve differently than in non-interacting quintessence cosmologies and, therefore, the interaction can be tested by its effects on the dynamical evolution of the Universe. Due to the interaction, the fraction of cold dark matter (CDM) at any time in the past is smaller than in non-interacting models with the same cosmological parameters today. Since the dark matter energy density grows more slowly the beginning of the period of accelerated expansion and the temporal evolution of the gravitational potential differ from non-interacting models. Observables such as the angular and luminosity distances depend on the time evolution of the energy density. But the effect does not only occurs at zeroth order; the evolution of first order matter density perturbations is also affected and so is the pattern of anisotropies of the CMB. This section describes the dynamical evolution of dark matter and dark energy densities at zeroth order in the interacting quintessence model of Ref. [15] to point out the main differences with respect to models with no interaction.

The phenomenological model of Chimento *et al.* [15] (see also [16]) assumes that the dark energy decays into cold dark matter thereby both energy densities do not longer evolve separately. In [18] the following ansatz was adopted

$$\dot{\rho}_c + 3H\rho_c = 3Hc^2(\rho_x + \rho_c), \quad \dot{\rho}_x + 3H(1 + w_x)\rho_x = -3Hc^2(\rho_x + \rho_c), \quad (1)$$

where  $\rho$  denotes the energy densities (subscript  $c$  for cold dark matter and subscript  $x$  for dark energy),  $w_x$  is the equation of state parameter of dark energy,  $H \equiv a^{-1}da/dt$  the Hubble function and  $a$  the scale factor of the flat Friedmann-Robertson-Walker metric. The model assumes that the dark energy decays just into cold dark matter and not into any other component such as neutrinos, baryons, or photons. Decay into neutrinos have been recently studied in the literature [19]. The coupling with baryons is constrained by measurements of local gravity [20, 21]. The above ansatz is essentially phenomenological; it is the simplest interaction model that leads to a constant ratio at early and late times which certainly alleviates the coincidence problem. While at present a rigorous derivation from first principles does not exist, the ansatz may be roughly justified as follows: the right hand side of both equations in (1) must be functions, say  $Q$  and  $-Q$ , of the energy densities multiplied by a quantity with units of inverse of time. For the latter the obvious choice is the Hubble factor  $H$ , so we have that  $Q = Q(H\rho_x, H\rho_c)$ . By power law expanding  $Q$  and retaining just the first term we get

$Q \simeq \lambda_x H \rho_x + \lambda_c H \rho_c$ . To facilitate comparison of the model with observation it is suitable to eliminate one of the two  $\lambda$  parameters. Thus we set  $\lambda_x = \lambda_c = 3c^2$  and arrive to Eq. (1). The simpler choice  $\lambda_c = 0$  would not yield a constant dark matter to dark energy ratio at late times. The dimensionless term  $3c^2$  measures to what extent the decay rate differs from the expansion rate of the Universe. Thus, the model is characterized by this single parameter,  $c^2$ , which also gauges the intensity of the interaction. The lower  $c^2$ , the closer the evolution of the Universe to a non-interacting model is.

Equations in (1), the continuity equations for photons and baryons and Friedmann equation  $H^2 = (\kappa^2/3)(\rho_{rad} + \rho_b + \rho_c + \rho_x)$ , constitute a closed system. In Fig. 1 we plot the evolution of the different matter density components: cold dark matter (thick solid line), dark energy (thin solid), photons (thin dot-dashed) and baryons (thick dot-dashed) for two values of the interaction parameter: left and right panels correspond to  $c^2 = 10^{-3}$  and  $c^2 = 0.1$ , respectively. In the figure we can see that Eqs. (1) have two asymptotic solutions with  $r = \text{constant}$ : at early times and in the immediate future. It is easy to prove that, in these two cases,  $r^2 + (w_x c^{-2} + 2)r + 1 = 0$  and the constant ratio is  $r_- = r(z \rightarrow \infty) \sim c^{-2}$  and  $r_+ = r(z \rightarrow 0) \sim c^2$ . These results represent a clear conceptual advantage with respect to the  $\Lambda$ CDM model. If the present acceleration of the Universe is generated by a cosmological constant, then the initial values of dark matter and cosmological constant have to be tuned by 96 orders of magnitude at Planck time, i.e.,  $r(t_{Planck}) = \Omega_m/\Omega_\Lambda \sim \mathcal{O}(10^{96})$ . In the model described above this ratio is fixed by the interaction rate,  $c^2$ . The initial condition problem is significantly alleviated. For example, if  $c^2 \sim 10^{-4}$  the initial dark matter to dark energy ratio will be  $r(t_{Planck}) \sim \mathcal{O}(10^4)$ .

To study the evolution of the corresponding autonomous system formed by the continuity equations of all energy components and Friedmann's equation we introduce the following set of variables,

$$x = \frac{\kappa}{H} \sqrt{\frac{\rho_x}{3}}, \quad y = \frac{\kappa}{H} \sqrt{\frac{\rho_c}{3}}, \quad z = \frac{\kappa}{H} \sqrt{\frac{\rho_b}{3}}, \quad u = \frac{\kappa}{H} \sqrt{\frac{\rho_{rad}}{3}}, \quad (2)$$

with  $\kappa = \sqrt{8\pi G}$ . Then, the dynamical equations can be recast as

$$\begin{aligned} x' &= \frac{1}{2} \left[ 3w_x (x^2 - 1) + u^2 - 3c^2 \left( 1 + \frac{y^2}{x^2} \right) \right] x, \\ y' &= \frac{1}{2} \left[ 3w_x x^2 + u^2 + 3c^2 \left( 1 + \frac{x^2}{y^2} \right) \right] y, \\ z' &= \frac{1}{2} [3w_x x^2 + u^2] z, \\ u' &= \frac{1}{2} [3w_x x^2 + u^2 - 1] u, \\ 1 &= x^2 + y^2 + z^2 + u^2, \end{aligned} \quad (3)$$

where a prime denotes derivative with respect to  $\ln a$ . As said above, the motivation for interacting quintessence models is to solve or, at least, ameliorate the coincidence problem. A solution will be achieved if the system (3) presents scaling solutions [22]. As already discussed, scaling solutions are characterized by a constant dark matter to dark energy ratio. Even more important are those scaling solutions that are also an attractor. In this way, the coincidence problem gets substantially alleviated because, regardless of the initial conditions, the system evolves toward a final state where the ratio of dark matter to dark energy stays constant.

In Table I we give the location of the four critical points of the autonomous system of Eqs. (3), their stability character and whether they give rise to accelerated or decelerated expansions. The first critical point,  $(x_-^2, y_-^2, 0, 0)$ , corresponds to the dark energy dominated epoch with

$$x_-^2 = \frac{1}{2w_x} \left( w_x - \sqrt{w_x^2 + 4c^2 w_x} \right), \quad y_-^2 = 1 - \frac{1}{2w_x} \left( w_x - \sqrt{w_x^2 + 4c^2 w_x} \right), \quad (4)$$

and it requires  $c^2 < |w_x|/4$ . As shown in [18], this coincides with the condition the interaction must fulfill to give a physically acceptable evolution for the Universe.

$(x_c^2, y_c^2, z_c^2, u_c^2)$	Existence condition	Stability character	Acceleration
$(x_-^2, y_-^2, 0, 0)$	$0 < c^2 <  w_x /4$	attractor	$\ddot{a} > 0$ if $w_x < -1/3$
$(x_+^2, y_+^2, 0, 0)$	$0 < c^2 <  w_x /4$	saddle point	$\ddot{a} < 0 \forall c^2, w_x$
$(0, 0, 1, 0)$	$\forall c^2, w_x$	unstable	$\ddot{a} < 0$
$(0, 0, 0, 1)$	$\forall c^2, w_x$	unstable	$\ddot{a} < 0$

TABLE I: Location of the critical points of the autonomous system of Eqs. (3), their stability and dynamical behavior of the Universe at those points.

The second critical point,

$$x_+^2 = \frac{1}{2w_x} \left( w_x + \sqrt{w_x + 4c^2 w_x} \right), \quad y_+^2 = 1 - \frac{1}{2w_x} \left( w_x + \sqrt{w_x + 4c^2 w_x} \right), \quad (5)$$

corresponds to the CDM dominated era and it is a saddle point.

The third critical point,  $(0, 0, 1, 0)$ , is unstable and physically unrealistic. It corresponds to a universe with just baryons (it contains neither radiation, nor matter, nor dark energy). Finally, the fourth point,  $(0, 0, 0, 1)$ , corresponds to the radiation dominated era and it is also unstable. To summarize, as soon as the other energy densities grow more important than radiation, the system moves away from this point, reaches a CDM dominated era, which corresponds to a saddle point, and eventually moves to a final attractor scaling solution in the dark energy dominated era. In a natural way, the dynamical evolution of the Universe is to asymptotically approach this attractor, a never-ending phase of accelerated expansion, in which the energy ratio  $r \equiv \rho_c/\rho_x$  remains constant.

### III. IQM AND THE COINCIDENCE PROBLEM

In [14] Amendola *et al.* discussed the conditions that interacting quintessence models must verify in order to solve the coincidence problem and have a correct sequence of cosmological eras -i.e., radiation, matter, and accelerated scaling solution. Many of the Lagrangians proposed in the literature do not correspond to acceptable scaling solutions. Those models either enter a phase of accelerated expansion right after the radiation epoch or present baryon dominated periods that would affect the growth of structure in the Universe. This brings about a great stress on the ability of a large class of models to explain or even ameliorate the coincidence problem.

The phenomenological model of Chimento *et al.* [15] is not affected by the results of Ref. [14] since the coupling between dark matter and dark energy is not of the type studied by Amendola *et al.*, namely,  $Q \propto \rho_m d\phi/d(\ln a)$ , where  $\rho_m$  denotes the dark matter energy density and  $\phi$  the scalar field. Equivalently, the Lagrangian associated to the effective potential given in Eq. (5) of Ref. [18] is not of the type described in [14]. As can be seen in Fig. 1 the model contains two scaling regime solutions, one in the radiation- and matter-dominated eras, another in the period of accelerated expansion -at late times. It reproduces the right succession of radiation, matter and accelerated epochs, each lasting long enough to give rise to the observed cosmic structure. It only remains to show under which circumstances there is not a baryon dominated period (as in left panel of Fig. 1) so that the formation of galaxies and large scale structure go unaffected.

#### A. Baryon dominated era

Some interacting quintessence models present the severe drawback that the Universe undergoes a baryon-dominated period prior to the DM era. This is rather problematic since CMB temperature anisotropies and the evolution of matter density perturbations would result largely affected. Unlike the models of Ref. [23], the

Chimento *et al.* model [15] does not have a stable baryon dominated era. To see this let us estimate when and for how long could the model we are considering undergoes a baryon dominated epoch. The maximum baryon energy density can be obtained by setting  $z' = 0$  in Eqs. (3). Noting that  $u^2 = -3w_x x^2$ , we have from the last equation in (3) that

$$z_{max}^2 = 1 - y^2 - (1 - 3w_x)x^2. \quad (6)$$

For  $r = \text{constant}$ ,  $r^2 + (w_x c^{-2} + 2)r + 1 = 0$ . To affect the growth of structure and the CMB temperature anisotropies, baryon domination should occur, if at all, well before the period of accelerated expansion, i.e., when  $1 \ll r \simeq r_+$  with  $r_+ = (1/2)[-(w_x c^{-2} + 2) + \sqrt{(w_x c^{-2} + 2)^2 - 4}] \simeq |w_x|c^{-2}$ . Since  $y^2 = r x^2$  Eq. (6) becomes

$$z_{max}^2 \simeq 1 - (1 + 3c^2)y^2. \quad (7)$$

Therefore, for an early baryon dominated era to have existed we must have  $z_{max}^2 \simeq 1 - (1 + 3c^2)y^2 > x^2 + y^2$ . Thus, bearing in mind that  $x^2 \ll y^2$  the condition for the said epoch to exist is

$$y^2 \leq \frac{1}{2 + 3c^2}. \quad (8)$$

A baryon dominated epoch may have occurred for  $c^2 \sim \mathcal{O}(10^{-1})$  or larger. However, this does not correspond to any stable critical point of the autonomous system and -as we shall see below- such high values of  $c^2$  are ruled out by the CMB data. Therefore, for  $c^2$  values of about  $10^{-2}$  or lower the model of Ref. [15] is free of a long period of baryon dominance.

To conclude, the succession of expansion eras in the model we are considering can be summarized as follows: after the initial radiation dominated era, the Universe might have gone through a very short baryon dominated period (if at all) followed by a DM dominated epoch (corresponding to an unstable critical point), to finally asymptotically approach a regime with a constant dark matter to dark energy ratio, at late times, in the accelerated expansion era.

#### IV. COMPARISON WITH OBSERVATIONAL DATA

The IQM of Ref. [15] evades the restrictions imposed by [14] and provides a viable model to explain the coincidence problem by means of cosmological scaling solutions. The actual existence of an interaction must be elucidated by contrasting the model with observations. In Refs. [18] and [24] we studied the effect of the interaction on the temperature anisotropies of the CMB, on matter power spectrum and on the luminosity distance. This opens up the possibility of using observational data to constrain the strength of the interaction -i.e., the  $c^2$  parameter-, at different redshifts. At present, data are available on the power spectrum of matter density perturbations extracted from galaxy catalogs [25, 26, 27], on temperature anisotropies ranging from the largest scales down to  $\sim 20$  arcmin [2] and on luminosity distances up to redshift  $z \sim 1$  measured using SNIa as standard candles [1]. Each data set probes the DE/DM coupling at different periods: CMB anisotropies at  $z \simeq 10^3$ , the slope of the matter power spectrum at  $z \leq 10^4$  and the luminosity distance test at  $z \sim 1$  and below. We carried out independent statistical analysis for each data set to see what constraints did the data impose on the interaction at different epochs.

The effect of the interaction on the various observables can be determined numerically only. Physically, the interaction renders the potential wells shallower in the matter dominated regime and matter density perturbations grow slower [24]; the gravitational pull on baryons prior to recombination weakens and the interaction alters the relative height of the acoustic peaks of the CMB spectrum and, finally, the interaction also changes the time evolution of the different energy densities, i.e., it affects the luminosity distance of standard candles.

$40 \leq H_0 \leq 100 \text{ km/s Mpc}^{-1}$	$0 \leq \Omega_c h^2 \leq 1$	$0 \leq \Omega_b h^2 \leq 1$	$-1 \leq w_x \leq -0.5$
$0.5 \leq n_s \leq 1.5$	$0.5 \leq A_s \leq 1.5$	$0.1 \leq e^{-2\tau} \leq 1.5$	$-9 \leq \log c^2 \leq -1$

TABLE II: Priors on different parameters for WMAP, SDSS data analysis. MCMCs are constrained to take values within those intervals. The amplitude of the matter power spectrum  $A_s = 1$  is the amplitude fixed by the COBE normalization.

Figure 2 shows these effects. In Figure 2(a)-2(c) we plot the matter, radiation power spectra, and the luminosity distance for three cosmological models with the parameters of WMAP 3yr data concordance model and interaction parameter  $c^2 = 0, 10^{-2}, 0.1$  corresponding to solid, dotted and long dashed lines, respectively. We also plot the data (see below) used in the statistical analysis. In Fig. 2(a), the effect of the interaction is to shift the matter radiation equality and strongly damp the slope of the matter power spectrum. As a result, a large interaction erases the matter power spectrum at small scales. In the figure, power spectra are normalized to Cosmic Microwave Background/Differential Microwave Radiometers (COBE/DMR). In Fig. 2(b) the interaction changes the relative height of the acoustic peaks. At low multipoles the amplitudes also differ, since the slower evolution of the potential at low redshift gives rise to an Integrated Sachs-Wolfe component of different amplitude. This effect is discussed in [32]. In Fig. 2(c) we see that the effect of the interaction is not very significant, and only when  $c^2$  is as high as  $\sim 0.1$  there is a tiny difference with non-interacting models that can be perceived at  $z \sim 2$ .

To constrain the model with observations, for every given set of cosmological parameters we generate the power spectrum of matter density perturbations and temperature anisotropies of the CMB using a modified version of the CMBFAST code [28]. Our cosmological models are described by the following parameters: dark matter, baryon and dark energy densities ( $\Omega_c, \Omega_b, \Omega_x = 1 - \Omega_c - \Omega_b$ ), dark energy equation of the state parameter ( $w_x$ ), Hubble constant ( $H_0$ ), amplitude and slope of the matter power spectrum at large scales ( $A_s, n_s$ ), interaction parameter ( $c^2$ ), and the epoch of reionization measured by the optical depth of the Universe to CMB photons ( $\tau$ ). We do not consider gravitational waves, massive neutrinos, or universes with curved spatial sections. Effectively, our parameter space is 8-dimensional. A brute force analysis of this parameter space would prove computationally very expensive. Instead, we chose to explore the parameter space using a Monte Carlo Markov chain (hereafter, MCMC) method, where the parameter domain is more heavily explored close to the best fit values. This method speeds up the calculation and at the same time explores fully the likelihood function and allows to determine accurately the model parameters and its error bars. We implemented the method as described in Ref. [29] which was first proposed by Gelman and Rubin [30]. For each data set we run 4 different MCMCs initiated at different regions of the parameter space. We followed the same practice than the WMAP team: the chain automatically stopped when a given degree of convergence ( $R \leq 1.2$  in the notation of [29]) was attained and when, at least, 40,000 models were computed.

### A. Constraints on IQMs from WMAP 3yr data

We run 4 MCMCs comparing models with WMAP 3yr data, using the same likelihood code than the WMAP team which is available at the Lambda Archive [33]. Table II shows the intervals where parameters are let to vary. These priors are conservative in the sense that they include all known measurements and we do not expect these limits to have any effect on our final results. Still, we first made a rough exploration of the parameter space to ensure that the maximum of the likelihood function remains far away from the surface of the parameter space volume, so the likelihood hypersurface is not affected by our priors. We stop the program when the chains have satisfied convergence and well-mixing criteria.

Figure 3 presents the joint confidence intervals at 68%, 95% and 99.9% for pairs of parameters after marginalizing over the rest. For convenience, the  $c^2$  axis uses a logarithmic scale and it has been cut at  $c^2 \leq 10^{-5}$ . In the figure, contours run parallel to the vertical axis, meaning that the data has only statistical power to set an upper limit on the interaction parameter. At the  $1\sigma$  confidence level,  $c^2 \leq 2.3 \times 10^{-3}$ . Figure 4 shows the same joint confidence contours for other pairs of parameters. In Table III we presents the best fit values of

Parameter	WMAP	SDSS
$c^2$	$\leq 2.3 \times 10^{-3}$	$\leq 4.8 \times 10^{-3}$
$\Omega_c h^2$	$0.105^{+0.009}_{-0.012}$	$0.24^{+0.23}_{-0.13}$
$10^2 \Omega_b h^2$	$2.22 \pm 0.07$	$3.0^{+1.8}_{-2.7}$
$w_x$	$\leq -0.90$	$\leq -0.6$
$H_0$	$71.3^{+1.2}_{-1.5}$	$\dots$
$n_s$	$0.94^{+0.04}_{-0.05}$	$0.85^{+0.15}_{-0.20}$
$\tau$	$0.09 \pm 0.04$	$\dots$

TABLE III: Mean values of cosmological parameters and their  $1\sigma$  errors obtained by fitting WMAP 3yr and SDSS LRGs data. For  $w_x$  only upper limits at the  $1\sigma$  confidence level are given. Values not quoted are weakly or not constrained by the data.

the cosmological parameters obtained from WMAP 3yr data alongside their  $1\sigma$  error bars. Those intervals are in rather good agreement with WMAP 3yr results: the values on  $\Omega_c h^2$  are slightly more uncertain and on  $H_0$  more precise. The small differences are to be expected due to our different sampling of the parameter space [31]. The main difference lies in  $w_x$ . For this parameter, we can only set upper limits. The reason is that we restricted our analysis to quintessence models,  $w_x \leq -1$ , and did not consider phantom models.

Let us remark that the shape of the likelihood function is not altered by the introduction of a new degree of freedom. It is well known that the CMB temperature anisotropies are highly degenerated and different combination of parameters give rise to very similar radiation power spectra. One would expect that one extra parameter would introduce extra degeneracies and modify the overall shape of the likelihood function. This is not the case and it simply reflects the fact that the best fit parameters are rather insensitive to the interaction (see Fig. 3). An obvious explanation is that WMAP data does not allow for large departures from non-interacting models. The interaction changes the depth of the potential wells at the last scattering surface but this effect cannot be counter-balanced by a suitable variation of other cosmological parameters. The maximum of the likelihood function is unaffected and the contours are not shifted.

### B. Constraints on IQMs from SDSS and 2dFRGS data

The matter power spectrum has been recently derived from two different galaxy catalogs: 2-degree Field Red Galaxy Survey (2dFRGS) [25], that comprises a sample of more than  $2 \times 10^5$  galaxies with measured redshifts, and the Luminous Red Galaxy sample (LRGs) of the Sloan Digital Sky Survey (SDSS) [26]. A larger study, using the SDSS Data Release 5, and comprising more than half a million galaxies showed similar results [27]. In [26], the power spectrum from the SDSS was computed producing uncorrelated minimum-variance measurements in 20  $k$ -bands of the clustering power and its anisotropy due to redshift-distortions, with narrow and well-behaved windows functions in the range  $0.01 h/\text{Mpc} < k < 0.2 h/\text{Mpc}$ . We used these data to fit the theoretical power spectrum,  $P(k)$ , calculated with a modified CMBFAST software and thus constrain the parameters of the cosmological model. Table II shows the priors imposed on the parameters in our MCMCs runs. In addition, we allowed the bias parameter to vary in the range  $0.5 < b < 2.5$ . We run 4 different MCMCs till the criteria of convergence and well mixing were met.

Figure 5 shows the joint confidence contours of  $c^2$  with other representative parameters. Like in Fig. 3, contours run almost parallel to the vertical axis. In Table III we give the cosmological parameters measured from this data set. We derived an upper limit of  $c^2 \leq 4.8 \times 10^{-3}$  at  $1\sigma$  confidence level. This constraint is weaker than the one provided by WMAP 3rd year data, but applies to a different range in redshift. This bound sets an upper limit on the value of  $c^2$  averaged over the whole length of the matter dominated epoch. Varying  $H_0$  or the total matter content changes the matter radiation equality and shifts the maximum of  $P(k)$  to larger scales, but it is around the maximum where the data have less statistical power. Matter and baryons change the amplitude and location of baryon acoustic oscillations but useful constraints can only be obtained by separating the physics of the oscillations from that governing the overall shape of the power spectrum [34] losing the information on the interaction. As a result, we obtained no useful constraints on cosmological parameters except on  $c^2$ . We

also run a set of MCMCs for the 2dFGRS data, but while the values of the main cosmological parameters were in very good agreement with those of Table III, the constraints were even poorer than those obtained from the SDSS data, so we do not present them here.

### C. Constraints from SNIa data

At low redshifts, only the dark matter and dark energy densities contribute substantially to the dynamical evolution of the Universe. Since the interaction alters their relative ratio, it affects the actual distance to objects. Distance measurements, like the luminosity distance,  $d_L$ , obtained from standard candles like the SNIa, are sensitive to the dark energy parameters,  $\Omega_x$ ,  $w_x$ , and the strength of the interaction,  $c^2$ . The likelihood function is given by [1],

$$\mathcal{L} \propto \exp\left(-\frac{1}{2}\chi^2\right), \quad \chi^2(H_0, w_x, \Omega_x, c^2) = \sum_i \frac{(\mu_{the}(z_i; H_0, w_x, \Omega_x, c^2) - \mu_{obs,i})^2}{\sigma_{\mu_{obs,i}}^2 + \sigma_v^2}. \quad (9)$$

In this expression,  $\mu = 5 \ln d_L + 25$  is the distance modulus,  $\sigma_v^2$  is the uncertainty on the supernova redshift (in units of the distance modulus) due to its intrinsic motion and the peculiar velocities of the parent galaxy and  $\sigma_{\mu_{obs,i}}^2$  is the error in the determination of the distance moduli due to photometric uncertainties. Subindexes *the* and *obs* indicate theoretical and observed uncertainties, respectively. Since the intrinsic luminosity of SNIa is not known, the distance moduli are insensitive to  $H_0$ , only 3 parameters ( $\Omega_x$ ,  $w_x$ , and  $c^2$ ) are needed to characterize a model. We carried out a brute force analysis sampling homogeneously the parameter space: ( $-9 \leq \log c^2 \leq -1$ ,  $0 \leq \Omega_x \leq 1$ ,  $-1 \leq w_x \leq -0.5$ ); each interval was subdivided in 10 steps. Figure 6 shows the confidence intervals for  $c^2$  vs  $\Omega_x$  after marginalizing over  $w_x$ . We remark that, in this case, the data is almost insensitive to  $c^2$ , as we could have expected from Fig 2(c).

### D. Bayesian model selection

To solve the coincidence problem a decay of DE into DM was postulated and, consequently, a new parameter,  $c^2$ , was introduced to gauge the strength of the coupling. In this subsection we explore whether the existence of this coupling (i.e., a non-vanishing  $c^2$  value) it is also justified by a statistical description of the data. The introduction of further parameters will lead to a better fit to the data. This must be balanced against the loss of predictive power of the theory. The Bayesian Information Criteria (defined as  $BIC = \chi^2 + k \log N$  [35], where  $\chi^2 = -2 \log \mathcal{L}$ ,  $k$  the number of free parameters, and  $N$  the number of data points), penalizes the inclusion of additional parameters to describe data of small size. For the WMAP 3yr data  $\chi^2(c^2 = 0) = 11252.06$  and  $\chi^2(\text{best model}) = 11251.85$ , so the interacting quintessence model for  $c^2 = 2.3 \times 10^{-3}$  yields a slightly better fit to data than the corresponding non-interacting model. However, the application of the Bayesian criterion gives  $BIC(\text{best model}) = 11269$  and  $BIC(c^2 = 0) = 11266$ , so the introduction of this parameter is not statistically encouraged. This results disagree with our analysis of WMAP 1yr data [18]. It was the unexpected consequence of our choice of priors: we fixed all models to agree with the COBE/DMR normalization. Since WMAP 1yr concordance model preferred a lower normalization, it was heavily penalized compared with interacting models. This discrepancy shows the importance of priors in Bayesian analysis. As argued in [36], model selection is not a substitute for parameter fitting; a lower BIC does not imply the data rejects interacting models, just makes them unlikely. However, they still have a theoretical advantage since they can help explain the coincidence problem, while non-interacting models cannot.



## V. CONCLUSIONS

Let us briefly point out that while the IQM model does not solve the coincidence problem in full (as it cannot predict the present ratio of dark matter to dark energy [37]) it substantially alleviates it. Indeed, if we take initial conditions at the Planck scale, in a model without interaction the ratio  $r$  at that epoch is about  $10^{96}$ . If  $c^2 \sim 10^{-3}$ , a value compatible with WMAP upper limit then, asymptotically,  $r(t \gg t_0) \sim 10^3$ , where  $t_0$  is the present time. Initially  $r(t \ll t_0) \sim 10^{-3}$ , so, while in a  $\Lambda$ CDM model the initial conditions have to be fine-tuned by 96 magnitude orders to get the present accelerated expansion, in the IQM the difference in orders of magnitude is just 6. A further advantage is that the model is not limited by the results of Ref. [14] since it successfully predicts that the Universe undergoes three successive cosmic eras of expansion, namely, radiation, matter and dark energy dominance. If the interaction parameter were  $c^2 \sim \mathcal{O}(10^{-1})$  or larger, it could undergo an era of baryon dominance, but this is not a stable solution and, in any case,  $c^2$  values larger than  $2.3 \times 10^{-3}$  do not appear compatible with CMB data.

The existence of a late accelerated expansion of the Universe requires  $w_x < -1/3$ , as in noninteracting models. Whether or not the present value of the ratio  $r$  coincides with the final attractor value depends on the parameters  $c^2$  and  $w_x$ . These are unknowns that can be constrained by observation. Our analysis shows that the CMB, matter power spectrum and luminosity distance data only set upper limits on the DM/DE coupling and, statistically, the introduction of this extra parameter is not favored by the data. At present, CMB data sets the tightest upper limit on the strength of the interaction ( $c^2 \leq 2.3 \times 10^{-3}$ ). As Fig. 7 reveals, this upper bound can be translated into an excluded region (shaded area) for the dark matter to dark energy ratio,  $r$ . Solid lines, from top to bottom, correspond to  $c^2 = 10^{-5}, 10^{-4}, 10^{-3}$  and  $2.3 \times 10^{-3}$  that bounds the shaded area. As the figure shows, the smaller  $c^2$ , the longer it takes to reach the attractor solution. With WMAP 3yr constraint, the attractor solution will be reached only in  $10^{11}$  yr from now. Our upper limits on  $c^2$  put pressure on this type of interacting models that, combined with the more generic results of [14], show the difficulties that interacting models encounter into explaining the coincidence problem. If the new WMAP 5yr data release sets an even stronger constraint on  $c^2$ , the IQM will loose much of its appeal.

## Acknowledgments

This research was partly supported by the Spanish “Ministerio de Educación y Ciencia” under Grants FIS2006-12296-C02-01, BFM2000-1322 and PR2005-0359, the “Junta de Castilla y León” (Project SA010C05) and the “Direcció General de Recerca de Catalunya” under Grant 2005 SGR 00087.

- 
- [1] A.G. Riess *et al.*, *Astrophys. J.* **607**, 665 (2004); P. Astier *et al.*, *Astron. Astrophys.* **447**, 31 (2006); W.M. Woodvasey *et al.*, arXiv:astro-ph/0701041.
  - [2] D.N. Spergel *et al.*, *Astrophys. J. Suppl* **170**, 377 (2007); G. Hinshaw *et al.*, *Astrophys. J. Suppl* **170**, 288 (2007).
  - [3] M. Colless *et al.*, *Mon. Not. R. Astron. Soc.* **328**, 1039 (2001); M. Tegmark *et al.*, *Phys. Rev. D* **69**, 103501 (2004); S. Cole *et al.*, *Mon. Not. R. Astron. Soc.* **362**, 505 (2005); V. Springel, C.S. Frenk, and S.M.D. White, *Nature (London)* **440**, 1137 (2006).
  - [4] S.P. Boughn, and R.G. Crittenden, *Nature* **427**, 45 (2004); S.P. Boughn, and R.G. Crittenden, *Mon. Not. R. Astron. Soc.* **360**, 1013, (2005); P. Fosalba, E. Gaztañaga, and F.J. Castander, *Astrophys. J.* **597**, L89 (2003); P. Fosalba, and E. Gaztañaga, *Mon. Not. R. Astron. Soc.* **350**, L37 (2004); J. D. McEwen, P. Vielva, M. P. Hobson, E. Martínez-González, A. N. Lasenby, *Mon. Not. R. Astron. Soc.* **376**, 1211 (2007); M.R. Nolta, *Astrophys. J.*, **608**, 10 (2004). P. Vielva, E. Martínez-González, and M. Tucci, *Mon. Not. R. Astron. Soc.* **365**, 891 (2006).
  - [5] C.R. Contaldi, H. Hoekstra, and A. Lewis, *Phys. Rev. Lett.* **90**, 221303 (2003).
  - [6] T. Padmanabhan, *Phys. Rep.* **380**, 235 (2003); V. Sahni, in *Lecture Notes in Physics* (Springer, Heidelberg, 2005) Vol. 653, p. 141; J.A.S. Lima, *Braz. J. Phys.* **34**, 194 (2004); L. Perivolaropoulos, *AIP Conf. Proc.* **848**, 698 (2006).
  - [7] E. Elizalde, *J. Phys. A. Math.Theor.* **40**, 6647 (2007).
  - [8] E.J. Copeland, M. Sami, and S. Tsujikawa, *Int. J. Mod. Phys. D* **15**, 1753 (2006).
  - [9] Jérôme Martin, private communication.

- [10] L. Amendola, M. Gasperini, and F. Piazza, *Phys. Rev. D* **74**, 127302 (2006).
- [11] C. Wetterich, *Nucl. Phys. B* **302**, 668 (1988); *Astron. Astrophys.* **301**, 321 (1995).
- [12] A. Coley and P. Bylliard, *Phys. Rev. D* **61**, 083503 (2000); G. Farrar and P.J.E. Peebles, *Astrophys. J.* **604**, 1 (2004); Y. Myung, *Phys. Lett. B* **626**, 1 (2005); R-G. Cai and A. Wang, *J. Cosmology Astropart. Phys.* 03(2005)002; S. del Campo, R. Herrera and D. Pavón, *Phys. Rev. D* **71**, 123529 (2005); B. Wang et al, *Phys. Lett. B* **624**, 141 (2005); D. Pavón and W. Zimdahl, *Phys. Lett. B* **628**, 206 (2005); B. Wang et al, *Phys. Lett. B* **637**, 357 (2006); H. Kim *et al.*, *Phys. Lett. B* **632**, 605 (2006); B. Hu and Y. Ling, *Phys. Rev. D* **73**, 123510 (2006); S. Lee, G.-C. Liu, and K.-W. Ng, *Phys. Rev. D* **73**, 083516 (2006); B. Guberina *et al.*, *J. Cosmology Astropart. Phys.* 01 (2007) 012; R. Horvath, *Phys. Lett. B* **648**, 374 (2007); M.S. Berger and H. Shojaei, *Phys. Rev. D* **74**, 043530 (2007); R. Mainini, and S. Bonometto, *J. Cosmology Astropart. Phys.* 06(2007)020; W. Zimdahl and D. Pavón, *Class. Quantum Grav.* **24**, 5461 (2007); O. Bertolami, F. Gil Pedro and M. Delliou, *Phys. Lett. B* (in the press), arXiv:astro-ph/0703462; E. Abdalla, L.R. Abramo, L. Sodre, and B. Wang, arXiv:0710.1198 [astro-ph].
- [13] F. Piazza and S. Tsujikawa, *J. Cosmol. Astropart. Phys.* **07** 004 (2004); B. Gumjudpai, T. Naskar, M. Sami and S. Tsujikawa, *J. Cosmol. Astropart. Phys.* **06**, 007 (2005).
- [14] L. Amendola, M. Quartin, S. Tsujikawa, and I. Waga, *Phys. Rev. D* **74**, 023525 (2006).
- [15] L.P. Chimento, A.S. Jakubi, D. Pavón, and W. Zimdahl, *Phys. Rev. D* **67**, 083513 (2003).
- [16] W. Zimdahl, D. Pavón, and L.P. Chimento, *Phys. Lett. B* **521**, 133 (2001).
- [17] Z.-K. Guo, N. Ohta, and S. Tsujikawa, *Phys. Rev. D* **76**, 023508 (2007).
- [18] G. Olivares, F. Atrio-Barandela, and D. Pavón, *Phys. Rev. D* **71**, 063523 (2005).
- [19] A.W. Brookfield, C. van de Bruck, D.F. Mota, and D. Tocchini-Valentini, *Phys. Rev. Lett.* **96**, 061301 (2006).
- [20] P.J.E. Peebles and B. Ratra, *Rev. Mod. Phys.* **75**, 559 (2003).
- [21] K. Hagiwara *et al.*, *Phys. Rev. D* **66**, 010001 (2002).
- [22] E.J. Copeland, A.R. Liddle, and D. Wands, *Phys. Rev. D* **57**, 4686 (1998).
- [23] D. Tocchini-Valentini and L. Amendola, *Phys. Rev. D* **65**, 063508 (2002); A.W. Brookfield, C. van de Bruck, D.F. Mota, and D. Tocchini-Valentini, *Phys. Rev. D* **73**, 083515 (2006).
- [24] G. Olivares, F. Atrio-Barandela, and D. Pavón, *Phys. Rev. D* **74**, 043521 (2006).
- [25] S. Cole *et al.*, *Month. Not. R. Astron. Soc.* **362**, 505 (2005).
- [26] M. Tegmark *et al.*, *Phys. Rev. D* **74**, 123507 (2006).
- [27] W.J. Percival *et al.*, *Astrophys. J.* **657**, 645 (2007).
- [28] <http://cfa-www.harvard.edu/~mzaldarr/CMBFAST/cmbfast.html>.
- [29] L. Verde *et al.*, *Astrophys. J. Suppl.* **148**, 195 (2003).
- [30] A. Gelman, and D. Rubin, *Statistical Science* **7**, 457 (1992).
- [31] A. Lewis, S. Bridle, *Phys. Rev. D* **66**, 103511 (2002).
- [32] G. Olivares, F. Atrio-Barandela, D. Pavón (2007). *Phys Rev D* (submitted).
- [33] <http://lambda.gsfc.nasa.gov/>
- [34] W.J. Percival *et al.*, *Astrophys. J.*, **657**, 51 (2007); W.J. Percival *et al.*, *Month. Not. R. Astron. Soc.* **381**, 1053 (2007).
- [35] G. Schwarz, *Annals of Statistics* **461**, 5 (1978); A.R. Liddle, *Month. Not. R. Astr. Soc.* **351**, L49 (2004).
- [36] E.V. Linder and R. Miquel, arXiv:astro-ph/0702542.
- [37] To best of our knowledge, no model predicts this value.

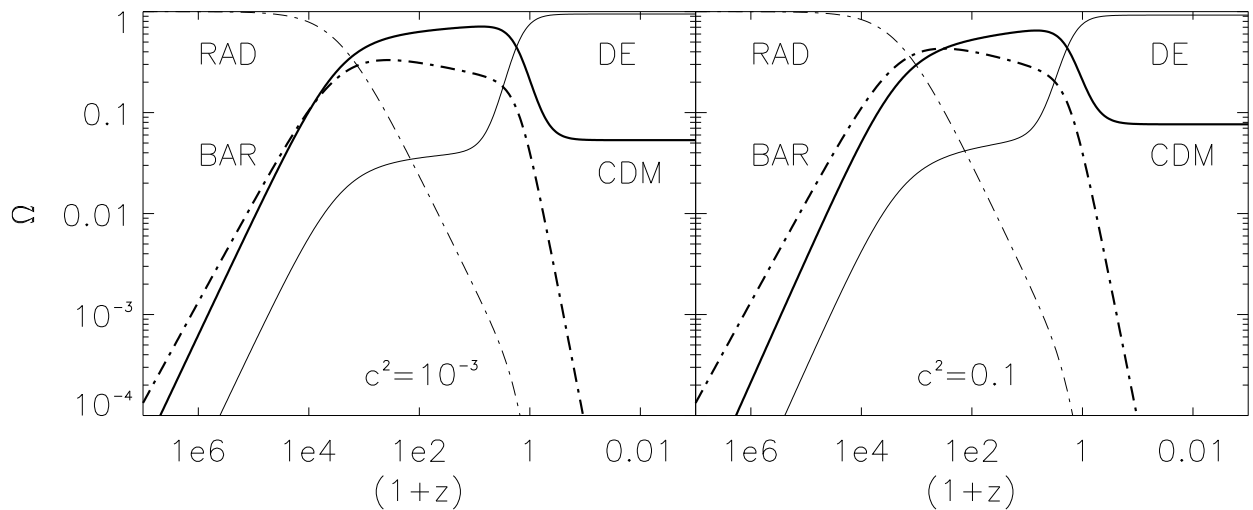


FIG. 1: Evolution of the different energy densities with redshift. Left panel:  $c^2 = 10^{-3}$ , right panel:  $c^2 = 0.1$ . Thick and thin solid, and thick, and thin dot-dashed lines correspond to dark matter, dark energy, baryons and photons, respectively.

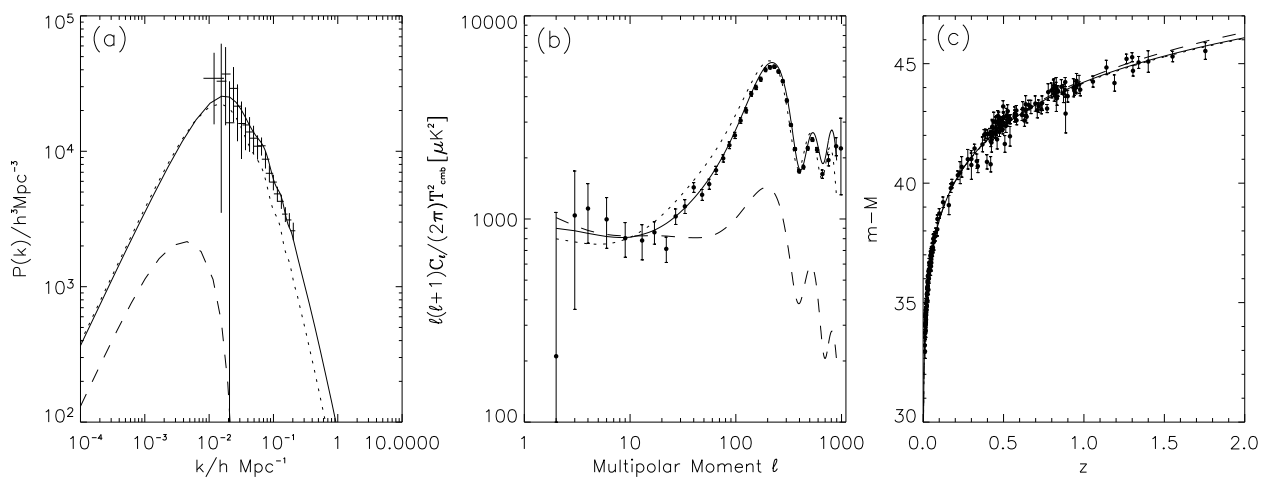


FIG. 2: Matter, radiation power spectrum, and luminosity distance for a cosmological model with  $\Omega_x = 0.74$  and  $w_x = -0.9$  and three different interaction parameters  $c^2 = 0, 10^{-2}, 0.1$ , corresponding to solid, dotted, and long dashed lines, respectively. The cosmological parameters are those of the fiducial WMAP 3yr data.

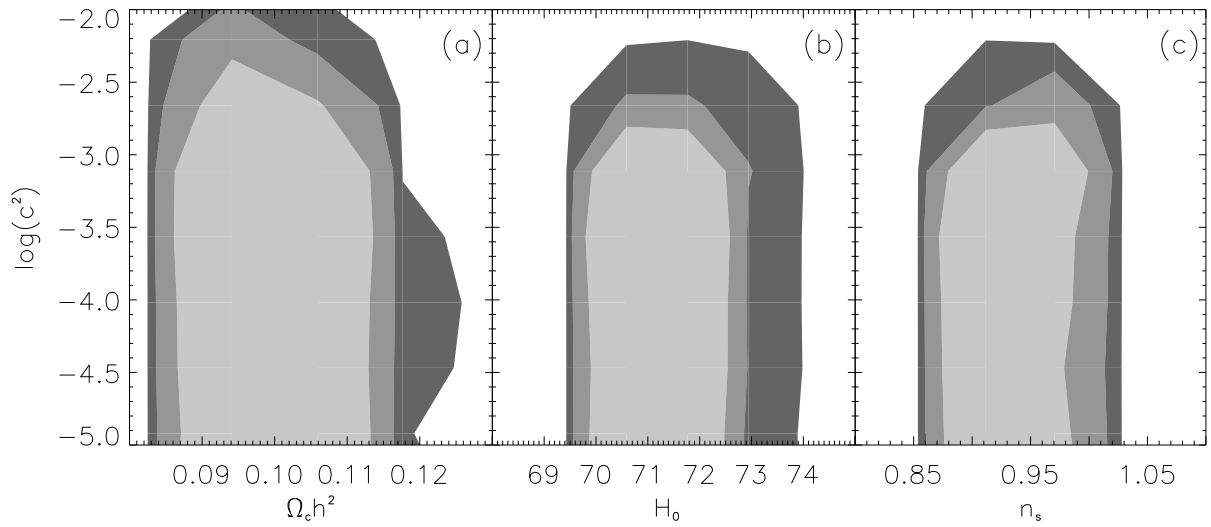


FIG. 3: Joint confidence intervals at the 68%, 95% and 99.9% level for pairs of parameters after marginalizing over the rest. For convenience, the  $c^2$  axis is represented using a logarithmic scale and it has been cut at  $c^2 \leq 10^{-5}$ .

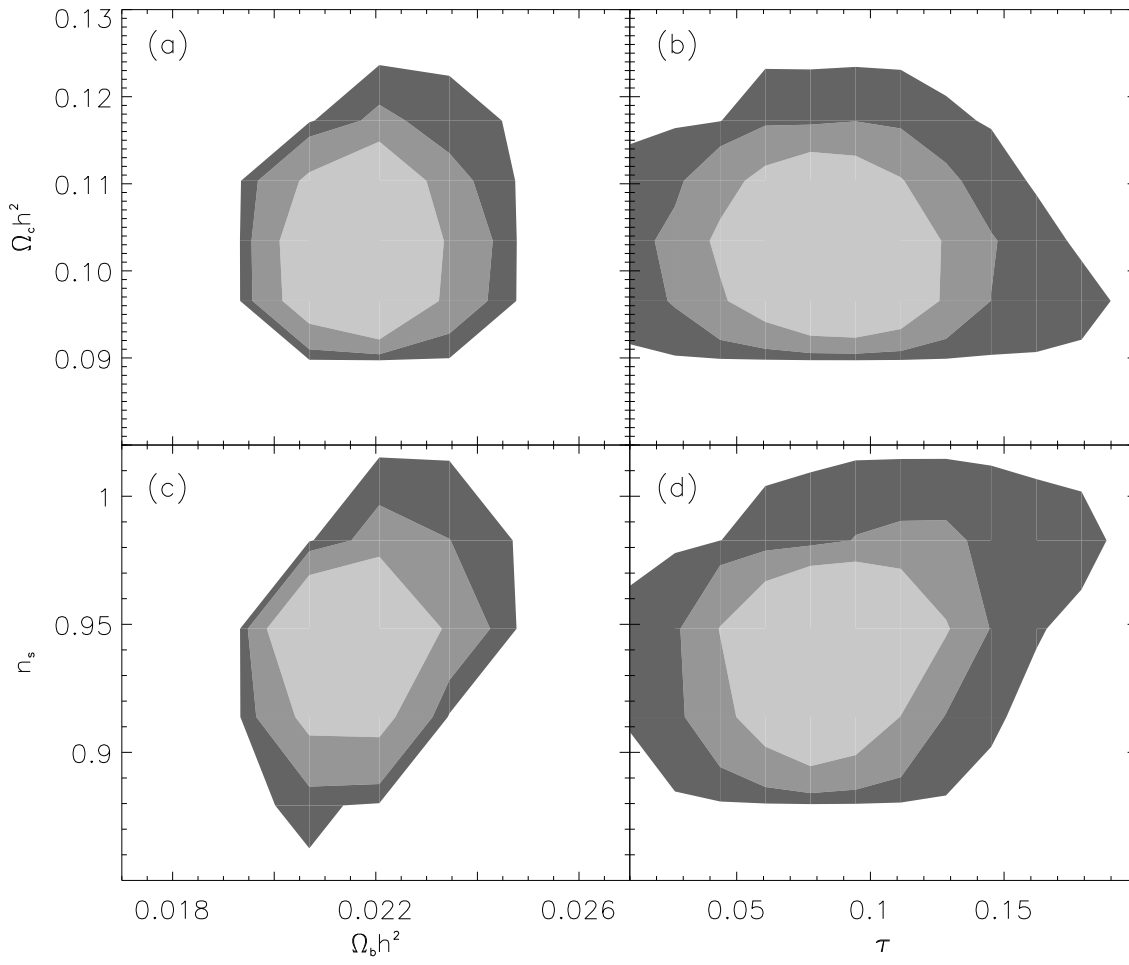


FIG. 4: Joint confidence intervals at the same confidence levels as in Fig. 3 for pairs of parameters after marginalizing over the rest.

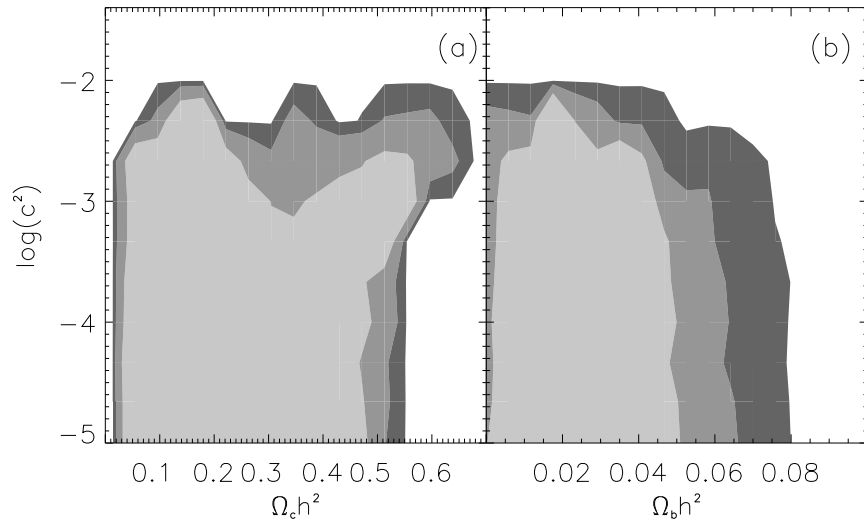


FIG. 5: Contours as in Fig. 3 obtained using the SDSS matter power spectrum data.

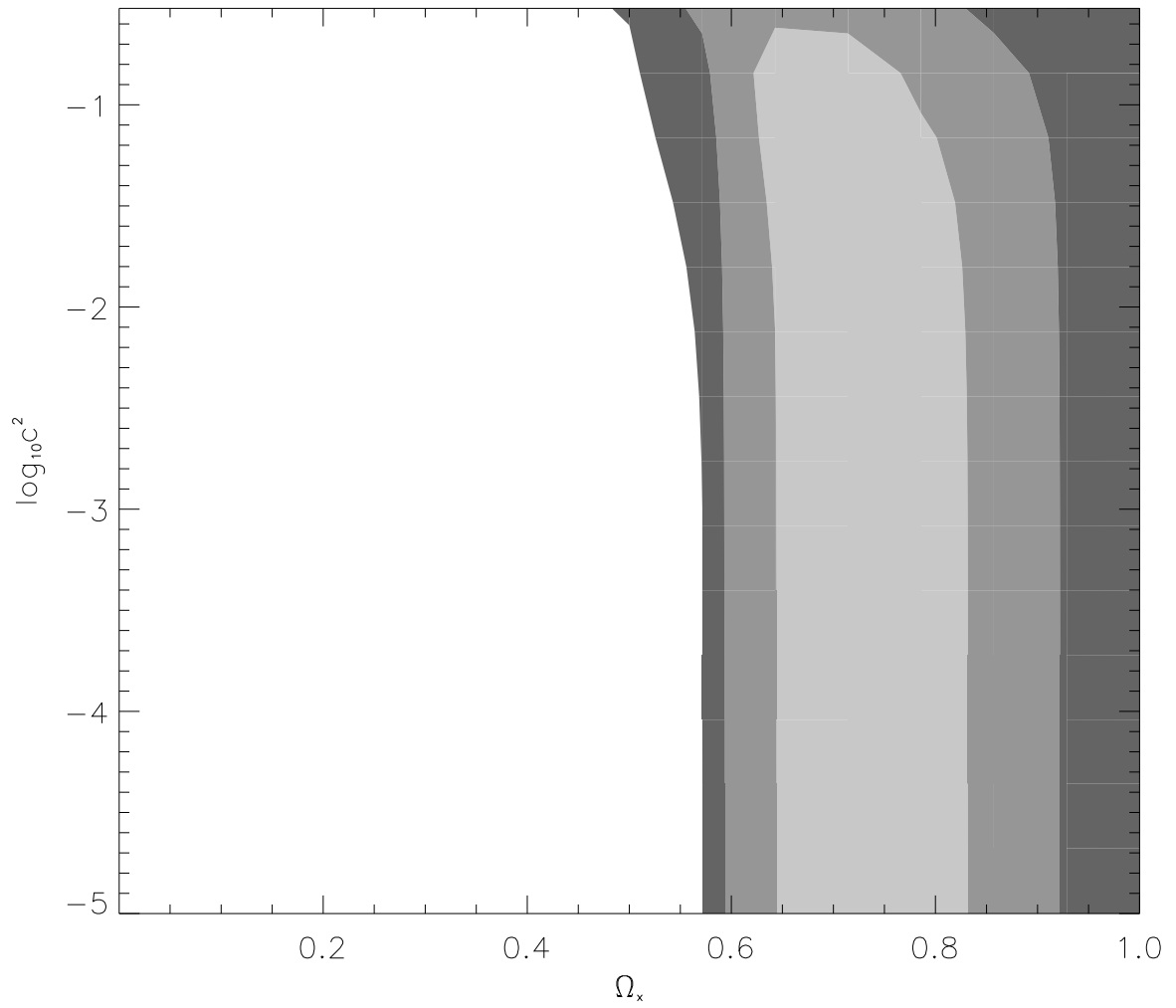


FIG. 6: Contours as in Fig. 3 obtained by fitting the luminosity distance IQM to the “Gold” sample of SNIa data of Riess *et al.* and SNLS data of Astier *et al.* [1].

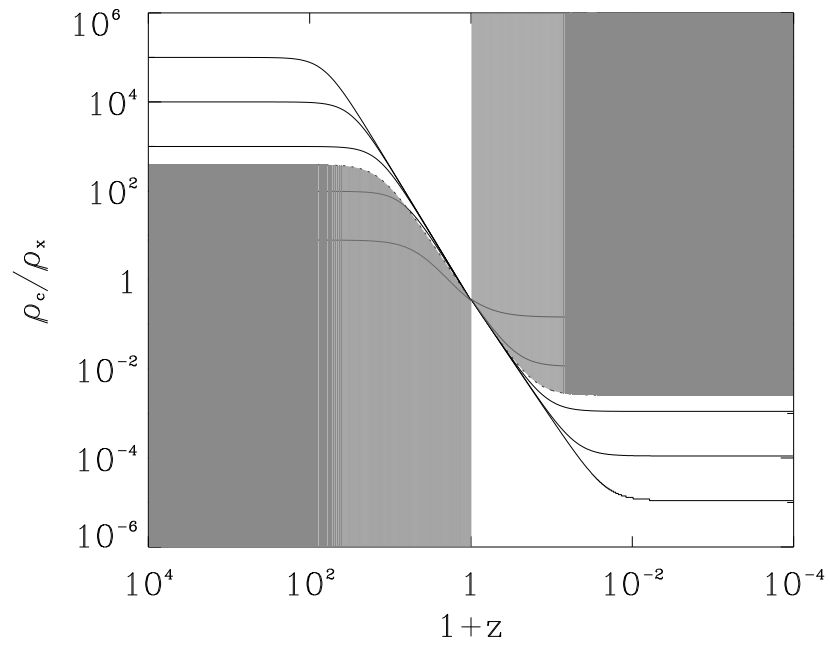


FIG. 7: Ratio DM/DE vs redshift. The  $c^2$  values on the curves from top to bottom (on the left hand side) are  $10^{-5}$ ,  $10^{-4}$ ,  $10^{-3}$ , and  $2.3 \times 10^{-3}$ . The shaded areas indicate the two regions excluded by the WMAP 3yr upper limit on  $c^2$ .